Monatsh Chem (2011) 142:599–608
DOI 10.1007/s00706-011-0503-9

ORIGINAL PAPER

Experimental and computational study on the reactivity of 2,3-bis[(3-pyridylmethyl)amino]-2(*Z*)-butene-1,4-dinitrile, a key intermediate for the synthesis of tribenzoporphyrazine bearing peripheral methyl(3-pyridylmethyl)amino substituents

Tomasz Goslinski · Zbigniew Dutkiewicz · Michal Kryjewski · Ewa Tykarska · Lukasz Sobotta · Wojciech Szczolko · Maria Gdaniec · Jadwiga Mielcarek

Received: 9 July 2010 / Accepted: 2 April 2011 / Published online: 4 May 2011

Abstract An earlier developed alkylating path leading to tetraalkylated diaminomaleonitrile derivatives was explored. Attempts to explain the reactivity of the representative dialkylated diaminomaleonitrile 2,3-bis[(3-pyridylmethyl)-amino]-2(*Z*)-butene-1,4-dinitrile during the alkylation reaction were performed using X-ray and density functional theory (DFT) studies. The condensed Fukui functions accompanied by softness indices were found to be useful in explaining its reactivity observed during the reaction. The values of the Fukui functions and condensed softness for electrophilic attack calculated from Mulliken, Löwdin, and natural population analyses closely corresponded to the experimental observations. When 2,3-bis[(3-pyridyl-methyl)amino]-2(*Z*)-butene-1,4-dinitrile disodium salt was treated with dimethyl sulfate at lower temperatures the alkylation reaction prevailed, whereas at higher temperatures the alkylating agent acted as a hydride anion acceptor, which favored the elimination reaction. The tetraalkylated dinitrile 2,3-bis[methyl(3-pyridylmethyl)amino]-2(*Z*)-butene-1,4-dinitrile was used in the synthesis of tribenzoporphyrazine bearing methyl(3-pyridylmethyl)amino groups, which was subsequently subjected to solvatochromic and metallation studies. The changes observed during metallation seem to result from the coordination of the 3-pyridyl group by a palladium ion. This could influence the configuration of the methyl(3-pyridylmethyl)amino moiety, causing more effective donation of a lone pair of electrons from peripheral nitrogen to the macrocyclic ring.

Keywords Alkylations · Density functional theory · Diaminomaleonitrile · Tribenzoporphyrazine · X-ray structure determination

Introduction

Diaminomaleonitrile (DAMN) and its derivatives have received much attention in recent years and have been extensively used in synthesis of amino-functionalized macrocycles and many other imine and imidazole compounds, pyrazines, pyrimidines, purines, azepines, pyrroles, oxazoles, nucleosides, and in photosynthesis of 4-amino-5-cyanoimidazole [1–7]. Tetraalkylated derivatives of DAMN are key substrates for synthesis of porphyrazines, including tribenzoporphyrazines bearing amino moieties. Peripheral amino groups provide these electron-rich macrocycles with unusual optical and electrochemical properties. They exhibit unusual coordination properties because of two metal ion binding sites—within the central cavity and by the peripheral amino moieties [3].

Porphyrins and related macrocycles, including porphyrazines bearing peripheral pyridyl substituents for self-assembly by metal ion coordination, have been widely

Electronic supplementary material The online version of this article (doi:10.1007/s00706-011-0503-9) contains supplementary material, which is available to authorized users.

T. Goslinski (✉) · Z. Dutkiewicz · E. Tykarska · W. Szczolko
Department of Chemical Technology of Drugs,
Poznan University of Medical Sciences, Grunwaldzka 6,
60-780 Poznan, Poland
e-mail: tomasz.goslinski@ump.edu.pl

M. Gdaniec
Faculty of Chemistry, Adam Mickiewicz University,
Grunwaldzka 6, 60-780 Poznan, Poland

M. Kryjewski · L. Sobotta · J. Mielcarek
Department of Inorganic and Analytical Chemistry,
Poznan University of Medical Sciences, Grunwaldzka 6,
60-780 Poznan, Poland

studied as molecular building blocks for creating supermolecular structures for potential use in nanotechnology [8, 9]. Many of the 2- and 4-pyridyl substituted macrocycles revealed excellent metal ion binding properties [10–13]. Methyl(2-pyridylmethyl)amino substituted tribenzoporphyrazines have shown excellent metal-binding abilities [3]. Macrocycles with a peripheral 3-pyridyl substituent have been little studied so far [14, 15], whereas porphyrazines substituted in the periphery with mixed methyl(3-pyridylmethyl)amino and 2,5-dimethylpyrrolyl ligands have revealed selective coordination properties [16]. In view of our work on synthesis and physicochemical studies of porphyrazines and tribenzoporphyrazines carrying peripheral methyl(3-pyridylmethyl)amino substituents, it appeared useful to investigate the spectroscopic properties of the metallated and unmetallated methyl(3-pyridylmethyl)amino moieties.

During the synthesis of a tetraalkylated DAMN derivative from a dialkylated precursor, undesired side-reactions took place, leading mainly to imine precursor formation. We further investigated this reaction in more detail using DFT studies. Imine product formation has been described in literature in various experiments performed on a dibenzyl DAMN derivative. Sheppard and coworkers have shown that 2,3-bis(benzylamino)-2(*Z*)-butene-1,4-dinitrile may be oxidized with 2,3-dichloro-5,6-dicyano-1,4-benzoquinone (DDQ) to dibenzyldiiminosuccinonitrile, which subsequently isomerizes to 2-benzylamino-3-benzylideneamino-2(*Z*)-butene-1,4-dinitrile [1]. Alkylation studies using a broad range of alkylating agents and bases, performed by Barrett, Hoffman, and coworkers on a dibenzyl DAMN derivative, indicated that in some reaction conditions this compound might act more like a hydride anion donor than a nucleophile. As a result, a reduced yield of tetraalkylated dinitrile, isolation of dinitrile isomers, or imine formation have been observed. Moreover, synthesis of imine has been noted during palladium-catalyzed alkylation of dibenzyl diaminomaleonitrile using methyl chloroacetate and the synthesis of acetic acid functionalized dibenzyl diaminomaleonitrile [4]. We aimed to address the cause of the reactivity of dialkylated DAMN derivatives and attempted to explain it using quantum chemical calculations.

Results and discussion

Synthesis

Sequential double-reductive alkylation of DAMN (**1**, Fig. 1) was employed to yield 2,3-bis[(3-pyridylmethyl)amino]-2(*Z*)-butene-1,4-dinitrile (**5**) following a method elaborated by the Sheppard [1] and Barrett–Hoffman teams [3]. The intermediates 2-amino-3-[(3-pyridylmethylidene)amino]-2(*Z*)-butene-1,4-dinitrile (**2**) and 2-amino-3-[(3-pyridylmethyl)amino]-2(*Z*)-butene-1,4-dinitrile (**3**) have been previously obtained and characterized [16]. It was found that alkylation reaction of **5** using dimethyl sulfate in the presence of sodium hydride in the temperature range −20 to −10 °C led to the alkylated 2,3-bis[methyl(3-pyridylmethyl)amino]-2(*Z*)-butene-1,4-dinitrile (**6**) with 13% yield. The product was isolated as red–brown oil, which was very unstable during attempted crystallization. Moreover, when the reaction was performed at 0 °C, imine 2-[(3-pyridylmethyl)amino]-3-[(3-pyridylmethylidene)amino]-2(*Z*)-butene-1,4-dinitrile (**4**) was isolated alone or in the mixture of products, yielding up to 45%. Attempts to elucidate this observation are reported later in this paper.

Linstead macrocyclization of tetraalkylated DAMN derivative **6** (magnesium butanolate in butanol) led in low yield to a symmetrical porphyrazine, which was hardly

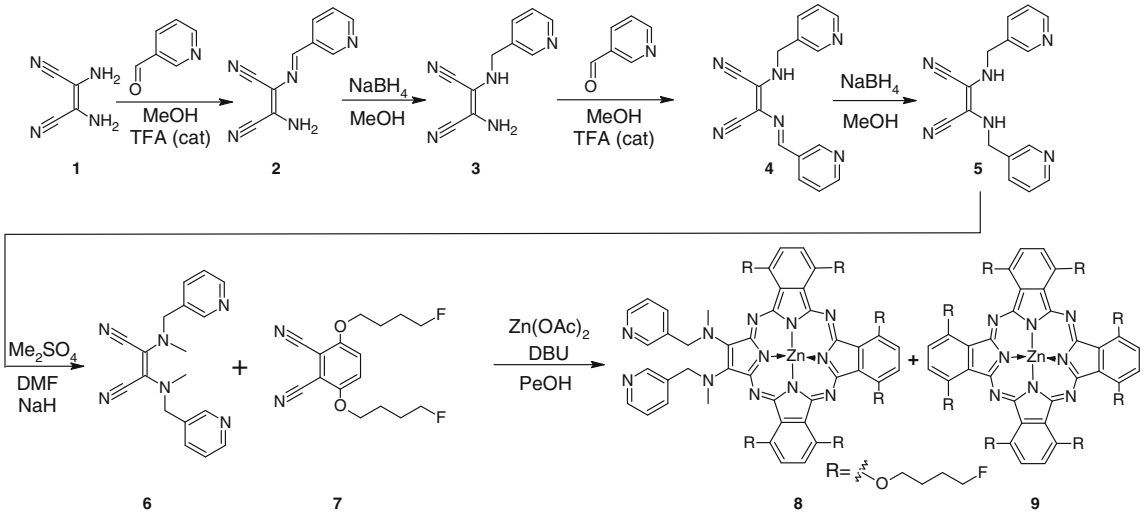

Fig. 1 Synthesis of dinitriles **4**–**6**, tribenzoporphyrazine **8**, and phthalocyanine **9**. *TFA* trifluoroacetic acid

soluble and therefore difficult to purify [17]. The new hydroquinone dialkyl ether 3,6-bis(4-fluorobutoxy)benzene-1,2-dicarbonitrile (**7**) was synthesized by modifying the method of 2,3-dicyanohydroquinone alkylation [18]. A mixed macrocyclization reaction of dinitriles **6** and **7** in pentanol using zinc acetate and 1,8-diazabicyclo[5.4.0]-undec-7-ene (DBU) as a base was employed to synthesize 1,4,8,11,15,18-hexakis(4-fluorobutoxy)-22,23-bis[methyl-(3-pyridylmethyl)amino]tribenzo[*b*,*g*,*l*]porphyrazinatozinc (II) (**8**) and [1,4,8,11,15,18,22,25-octakis(4-fluorobutoxy)-phthalocyanato]zinc(II) (**9**). Compound **8** appeared to possess good solubility in common organic solvents due to the presence of lipophilic 4-fluorobutoxy groups in nonperipheral positions. The structures of tribenzoporphyrazine **8** and phthalocyanine **9** were elucidated using nuclear magnetic resonance (NMR) data and are discussed in the Supplementary Material.

*Attempts to explain the alkylation reaction of **5** on the basis of crystal structure analysis and quantum chemical calculation*

The imine product formation observed during the course of experiments was explained by crystal structure analysis of dinitriles **4** and **5** and quantum chemical calculations of dinitrile **5**. The structures of both dinitriles **4** and **5** determined by X-ray crystallography (Fig. 2) show that the chemical modification from the imine group in **4** to the amine group in **5** had virtually no effect on the crystal packing and molecular conformations, as the crystals of these two compounds are isostructural.

In compounds **4** and **5** the amino N atom in part A has planar sp^2 hybridization and all atoms bonded to N8A are coplanar with the maleonitrile fragment [the torsion angle C7A-N8A-C2-C3 is −173.6(1)° and −171.4(1)° for **4** and **5**, respectively]. Thus, there is significant involvement of the amino N lone pair of electrons with the π-system of the maleonitrile unit, which results in shortening of the formally single N8A-C2 bond [the bond distance is 1.346(2) Å in **4** and 1.359(1) Å in **5**]. In the chemically symmetrical compound **5** both parts, A and B, of the molecule are structurally different, because the amino N8B atom in part B has sp^3 hybridization. The sp^2 hybridization of the two amino N atoms would result in steric hindrance between the two amino hydrogens, and the relief of the strain in **5** is achieved by pyramidalization of one of the enamine N atoms (N8B), giving rise to the reduction of conjugation between the electron lone pair of the amino nitrogen and the double-bond π electrons. This fact is reflected in a significant lengthening of the Csp^2-N bond to this amino group [C3-N8B 1.408(2) Å]. In compound **4** the π-electron delocalization occurs over a larger part of the molecule than in **5** because it additionally includes the imine –N=C– fragment and the pyridine ring. In **4** the imine group is conjugated not only with the maleonitrile fragment but also with the pyridine ring, and this explains why the corresponding Csp^2-Nsp^2 and Csp^2-Nsp^3 bond

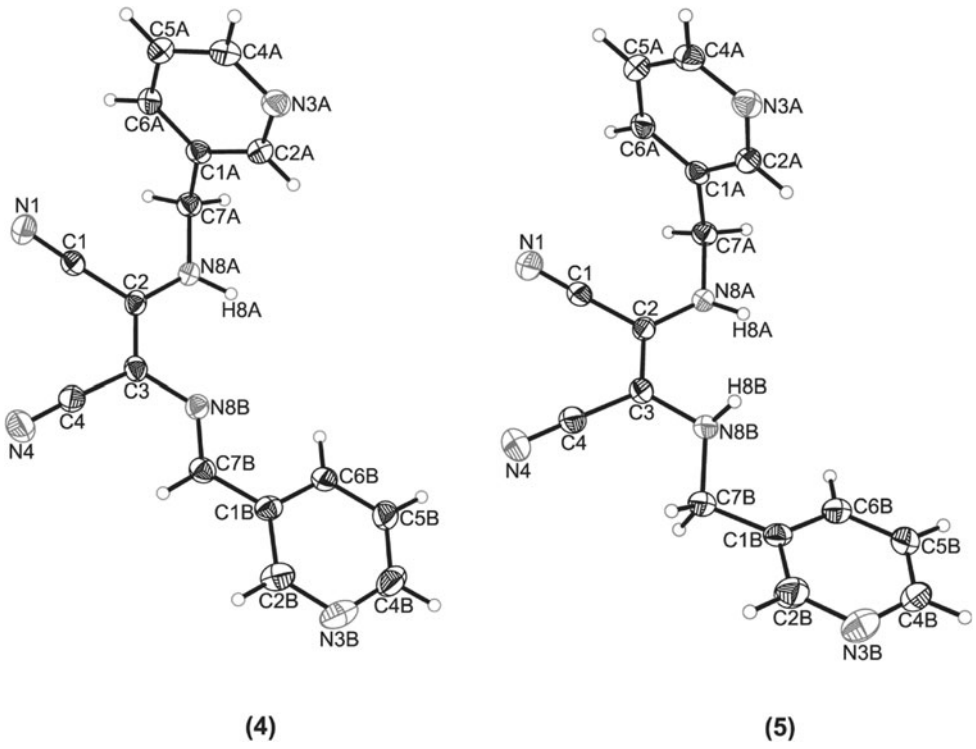

Fig. 2 X-ray structures of dinitriles **4** and **5** showing the atom-labeling scheme. Displacement ellipsoids are drawn at the 50% probability level, and H atoms are shown as spheres of arbitrary radius

lengths in **4** and **5** are virtually the same [C3-N8B 1.392(2) Å in **4** and 1.408(2) Å in **5**].

X-ray data showing inequivalence of the two sides of dinitrile **5** in the solid state have pleasingly corresponded to literature quantum mechanical calculations of the rotational barriers in diaminomaleonitrile performed by Dwyer et al. [19]. DAMN is able to achieve stability by rotating one amino group of the heavy atom plane by 90° so that the amino hydrogens lie above and below the aforementioned plane and conjugating a single N lone pair into the C=C π system. What has been found interesting in the minimum-energy structure of DAMN is that the amino nitrogens are pyramidal and the C–N bond of the twisted amino group is 0.04 Å longer than the C–N bond which is coplanar with the maleonitrile part. The minimum-energy structure of DAMN implies that the most stable geometry involves delocalization of a lone pair from a single nitrogen. We consider that this may generally explain the observed inequivalence of the two DAMN amine groups during reductive alkylation and force the sequential double-reductive alkylation of DAMN in the synthetic path.

Our DFT studies were performed in order to explore the reactivity of **5** during alkylation reaction. Optimizations of molecular structures of **5** in the form of its disodium salt (**5-Na**) at the B3LYP/6-31G(d,p) level were preceded by conformational study of **5** in vacuo at the B3LYP/6-31G(d,p) level. As a result of this search, more than 100 conformations were found for **5**, in which 26 groups of conformers were identified. These conformers possessed dihedral angles of very similar values within the same group: α_1 (C3-C2-N8A-C7A), α_2 (C2-C3-N8B-C7B), β_1 (C2-N8A-C7A-C1A), β_2 (C3-N8B-C7B-C1B), and four different sets of angles describing 3-pyridyl ring rotation γ_1 (N8A-C7A-C1A-C6A) and γ_2 (N8B-C7B-C1B-C6B). In almost all conformations the molecular frame (DAMN moiety with CH_2 groups) was found to possess C_1 symmetry, with the exception of two conformations for which C_2 symmetry appeared and the other two for which the symmetry of the molecular frame was very close to C_2 (the same group of four conformations with similar values of α_1, α_2, β_1, and β_2).

In the next step, three conformations of **5** found in the conformational study were selected: the unsymmetrical conformation with the lowest energy (C_1 symmetry), another unsymmetrical conformation (the energy of which is higher than that found for the previous conformation but lower than that of the optimized X-ray structure), and a symmetrical conformation (C_2 symmetry). The optimized X-ray structure of **5** was selected as the fourth conformation for further study. Hydrogen atoms H8A and H8B in these four conformers of dinitrile **5** were replaced with sodium atoms to give the corresponding sodium salts (**5-Na1–5Na4**), which were subsequently optimized in the gas phase. These optimizations were followed by vibration frequency calculations to ensure that all four conformations were true minima on the potential-energy surface (Table 5S, Supplementary Material).

The condensed Fukui functions were applied to explain both reaction paths observed during alkylation reaction of **5**, one being alkylation to **6** and the other being formation of imine **4**. The selected values for the Fukui functions f_k^-, f_k^+, and f_k^0 and condensed softness $s_k^-(s_k^- = Sf_k^-)$ for electrophilic attack were calculated from Mulliken (MPA), Löwdin (LPA), and natural population (NPA) analyses and are presented in Table 1 (complete data Tables 6S–9S, Supplementary Material) [20].

DFT calculations indicate that both sides of dinitrile disodium salt **5-Na** are identically or almost identically traceable for alkylating agents (Fig. 3). The values of the s_k^- indices for N8A and N8B are in the ranges 0.159–0.477, 0.234–0.723, and 0.559–1.093 in accordance with MPA, LPA, and NPA analyses, respectively. What is interesting is that these indices obtained using MPA, LPA, and NPA analyses for H71A, H72A, H71B, and H72B had the following values: 0.102–0.293, 0.044–0.172, and 0.057–0.209. These condensed softness values clearly indicate the overall tendency of the alkylation reaction to be dominant (s_k^- values for N8A and N8B), which is particularly pronounced in the NPA and LPA analyses. Nevertheless, it might be presumed that, at higher temperature, especially for unsymmetrical conformers, the elimination reaction might take place (s_k^- values for H71A, H72A and H71B, H72B). Moreover, the overall tendency for the elimination reaction to proceed, based on the ratios of s_k^- values for H71A, H72A to N8A and H71B, H72B to N8B, is more marked for unsymmetrical conformers than for symmetrical ones (Table 10S, Supplementary Material).

The calculated data pleasingly correspond to the experimental observations. When dinitrile **5-Na** was treated with dimethyl sulfate at lower temperature the alkylation reaction prevailed, whereas at higher temperature the alkylating agent acted as hydride anion acceptor, which favored the elimination reaction.

Spectroscopic and solvatochromic studies

Since the heteroatoms present at the β positions of porphyrazines and tribenzoporphyrazines are in direct electronic contact with the macrocyclic core π system, the binding of metal ions is evidenced by profound changes in their UV–Vis spectra. The research previously performed on metalloporphyrazines functionalized with heteroatoms coordinating additional metal ions has opened the way to the applications of these compounds as sensors, which have been demonstrated so far for, e.g., pzs bearing peripheral

Table 1 Condensed Fukui functions and softness indices s_k^- for **5-Na** calculated from Mulliken, Löwdin, and natural population analyses at B3LYP/6-31G(d,p) level

	5-Na1	5-Na2	5-Na3	5-Na4		5-Na1	5-Na2	5-Na3	5-Na4
MPA f^- (S^-)									
N8A	0.089	0.091	0.070	0.067	N8B	0.036	0.032	0.070	0.067
	(0.477)	(0.454)	(0.364)	(0.360)		(0.195)	(0.159)	(0.363)	(0.361)
C7A	−0.048	−0.030	−0.030	−0.029	C7B	−0.039	−0.034	−0.030	−0.029
	(−0.257)	(−0. 150)	(−0.157)	(−0.158)		(−0.208)	(−0.171)	(−0.158)	(−0.158)
H71A	0.053	0.055	0.048	0.048	H71B	0.047	0.047	0.044	0.048
	(0.285)	(0.273)	(0.249)	(0.256)		(0.251)	(0.234)	(0.228)	(0.256)
H72A	0.055	0.040	0.044	0.043	H72B	0.035	0.020	0.048	0.043
	(0.293)	(0.202)	(0.228)	(0.230)		(0.188)	(0.102)	(0.249)	(0.230)
LPA f^- (S^-)									
N8A	0.135	0.134	0.106	0.100	N8B	0.057	0.047	0.106	0.100
	(0.723)	(0.668)	(0.550)	(0.536)		(0.305)	(0.234)	(0.548)	(0.537)
C7A	−0.001	0.003	0.002	0.002	C7B	0.006	0.009	0.002	0.002
	(−0.007)	(0.013)	(0.009)	(0.013)		(0.031)	(0.044)	(0.009)	(0.013)
H71A	0.030	0.029	0.022	0.022	H71B	0.022	0.021	0.023	0.022
	(0.159)	(0.145)	(0.114)	(0.118)		(0.116)	(0.105)	(0.118)	(0.118)
H72A	0.032	0.019	0.023	0.022	H72B	0.017	0.009	0.022	0.021
	(0.172)	(0.094)	(0.118)	(0.116)		(0.089)	(0.044)	(0.114)	(0.116)
NPA f^- (S^-)									
N8A	0.204	0.195	0.191	0.185	N8B	0.128	0.112	0.191	0.185
	(1.093)	(0.973)	(0.993)	(0.997)		(0.687)	(0.559)	(0.991)	(0.997)
C7A	−0.027	−0.020	−0.022	−0.021	C7B	−0.018	−0.010	−0.022	−0.021
	(−0.146)	(−0.102)	(−0.113)	(−0.113)		(−0.096)	(−0.051)	(−0.113)	(−0.113)
H71A	0.036	0.034	0.027	0.027	H71B	0.027	0.028	0.028	0.027
	(0.192)	(0.170)	(0.139)	(0.143)		(0.144)	(0.138)	(0.144)	(0.143)
H72A	0.039	0.022	0.028	0.026	H72B	0.022	0.011	0.027	0.026
	(0.209)	(0.112)	(0.144)	(0.142)		(0.115)	(0.057)	(0.138)	(0.141)

Softness indices (in au^{-1}) are given in parentheses

diaza-18-crown-6 ring systems and *N*-methyl-(2-pyridylmethyl)amino units [3, 21].

UV–Vis spectroscopy was employed to evaluate solvatochromic effects of **8** and **9**. In dichloromethane:methanol (1:1) solution, tribenzoporphyrazine **8** exhibits a Soret peak at 332 nm and Q-band at 730 nm with shoulders at 660 and 810 nm. Solvatochromic studies performed on **8** (Fig. 4) and **9** (Fig. 11S, Supplementary Material) in various aprotic and protic solvents revealed the Q-band changes in the range from 723 nm (acetonitrile) to 736 nm (pyridine) [22, 23]. The Q-band wavelength is better correlated to the refractive index than the dipole moment for **8** and **9** (Table 2), suggesting that the red-shift is due to solvation rather than coordination.

Tribenzoporphyrazine **8** was further subjected to titration with palladium ions, showing significant changes in the UV–Vis profile, probably due to heterobimetallic porphyrazine product formation carrying the exocyclic di(3-pyridylmethyl)-$PdCl_2$ bonded fragment. Titration with Pd(II) resulted in a less intensive decrease in the Soret band and a more intensive Q-band absorption that continued through a Pd(II)-ligand ratio of ca. 1 (Fig. 4). Additionally a large red-shift of the Q-band by 120 nm together with a shift of the n-π^* peak to ca. 560 nm were observed. We propose that the changes observed during metallation are due to the coordination of the 3-pyridyl group by a palladium ion, which may change the configuration of the methyl(3-pyridylmethyl)amino moiety, causing more effective donation of a lone pair of electrons from peripheral nitrogen to the macrocyclic ring. This proposition is based on the fact that the n-π* band in the UV–Vis spectrum of tribenzoporphyrazine did not occur before, but after the metallation. Unfortunately, this complex appeared to be very sensitive to light and oxygen, as its photobleaching slowly occurred and it was not possible to obtain crystals suitable for X-ray measurements.

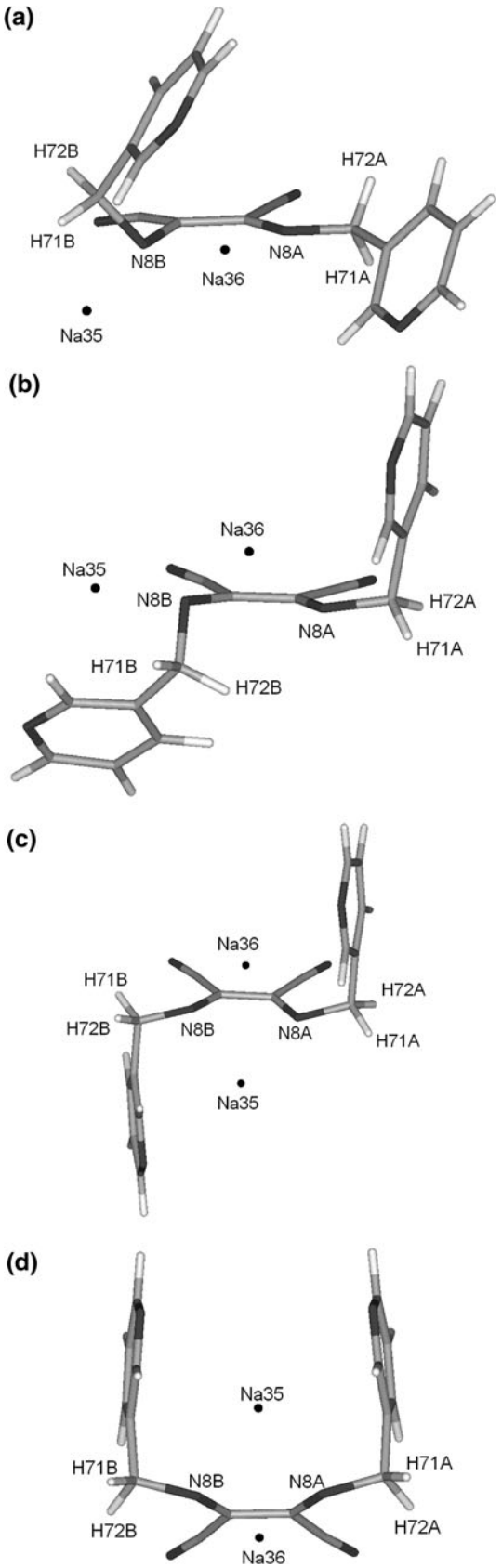

Fig. 3 Optimized structures of dinitrile **5-Na** derived from: **a** the ▶ lowest-energy conformation of dinitrile **5-Na1**; **b** one of the C_1-symmetry conformations of dinitrile **5-Na2**; **c** one of the C_2-symmetry conformations of dinitrile **5-Na3**; **d** optimized X-ray conformation of dinitrile **5-Na4**

Conclusions

A previously developed alkylating path leading to tetraalkylated diaminomaleonitrile derivatives was examined. An attempt to explain the reactivity of the representative dialkylated diaminomaleonitrile 2,3-bis[(3-pyridylmethyl)amino]-2(*Z*)-butene-1,4-dinitrile during alkylation reaction was performed using X-ray and DFT studies. The condensed Fukui functions accompanied by softness indices appeared to be useful in the explanation of both routes of the observed alkylation reaction. The values of the Fukui functions and condensed softness for electrophilic attack calculated from Mulliken, Löwdin, and natural population analyses closely correspond to the experimental observations. When 2,3-bis[(3-pyridylmethyl)amino]-2(*Z*)-butene-1,4-dinitrile disodium salt was treated with dimethyl sulfate at lower temperatures the alkylation reaction prevailed, whereas at higher temperatures the alkylating agent acted as hydride anion acceptor, which favored the elimination reaction. The tetraalkylated dinitrile 2,3-bis[methyl(3-pyridylmethyl)amino]-2(*Z*)-butene-1,4-dinitrile was used in the synthesis of tribenzoporphyrazine bearing methyl(3-pyridylmethyl)amino groups, which was subsequently subjected to solvatochromic and metallation studies. The changes observed during metallation appear to result from the coordination of the 3-pyridyl group by a palladium ion, which could influence the configuration of the methyl(3-pyridylmethyl)amino moiety, causing more effective donation of a lone pair of electrons from peripheral nitrogen to the macrocyclic ring.

Experimental

All reactions were conducted in oven-dried glassware under nitrogen. Reaction temperatures reported refer to external bath temperatures. Methanol and dichloromethane were distilled. Other solvents and all reagents were obtained from commercial suppliers and used without further purification. Melting points were obtained on a "Stuart" Bibby Sterlin Ltd.® melting point apparatus. All solvents were evaporated at or below 50 °C. Chromatography was carried out on Merck silica (eluents are given in parentheses). Dry flash column chromatography was carried out on silica gel 60, particle size 40–63 μm. Thin-layer chromatography (TLC)

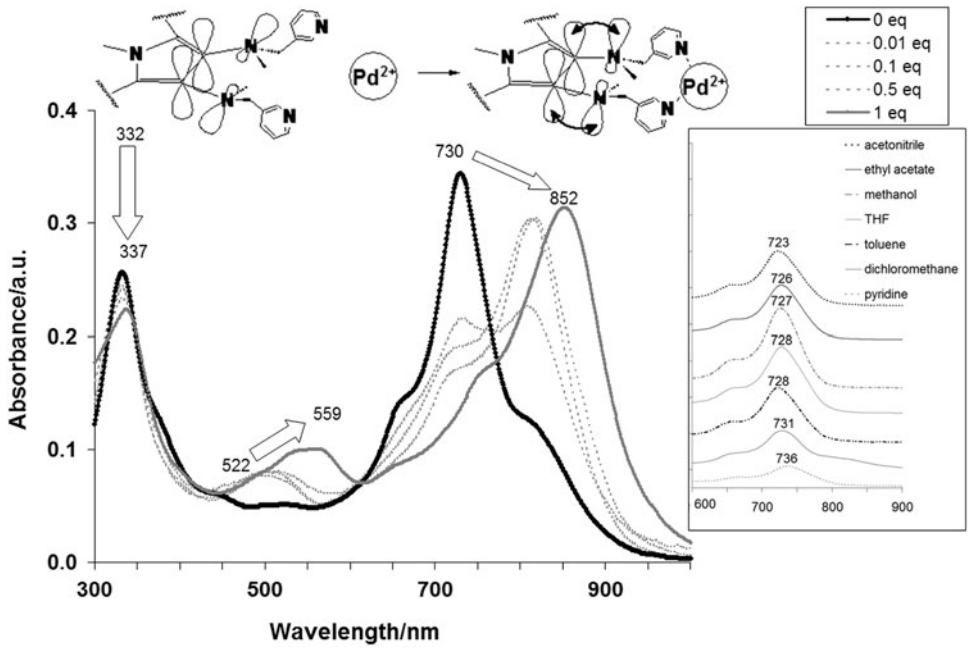

Fig. 4 Tribenzoporphyrazine **8** (*black line*) titrated with $PdCl_2(PhCN)_2$ in dichloromethane:methanol (1:1). Variations of the Q-band in different solvents (inset)

Table 2 Variations of the Q-bands for **8** and **9** in different solvents

Solvent	Dipole moment (μ)	Refractive index (n_D)	Q-band (λ_{max}, nm) **8**	Q-band (λ_{max}, nm) **9**
Acetonitrile	3.92	1.344	723	661, 733
Ethyl acetate	1.78	1.372	726	730, 799
Methanol	1.70	1.328	727	662, 736
THF	1.75	1.407	728	658, 732
Toluene	0.37	1.497	728	741, 803
Dichloromethane	1.60	1.455	731	760, 807
Pyridine	2.21	1.510	736	666, 742

was performed on silica gel Merck Kieselgel 60 and 60 F_{254} plates. UV–Vis spectra were recorded on a Hitachi UV/VIS U-1900 spectrometer. ^1H and ^{13}C NMR spectra were recorded on Varian Unity 300 FT and Bruker DRX-400 spectrometers. Chemical shifts (δ) are quoted in parts per million (ppm) and are referred to a residual solvent peak. Coupling constants (J) are quoted in Hertz (Hz) to the nearest 0.5 Hz. The abbreviations s, d, t, p, m, and Ar refer to singlet, doublet, triplet, pentet, multiplet, and aromatic, respectively. Additional techniques [^1H-^1H correlation spectroscopy (COSY), heteronuclear multiple quantum coherence (HMQC), heteronuclear multiple bond coherence (HMBC)] were used to assist allocation. Analytical high-performance liquid chromatography (HPLC) was performed on an Agilent 1200 instrument using Agilent Eclipse XDB-C18 (150 × 4.6 mm, 5 μm) column. Low- and high-resolution mass spectrometry [chemical ionization (CI), electrospray ionization (ESI), matrix-assisted laser desorption/ionization (MALDI) time of flight (TOF)] were recorded by both the Imperial College London Department of Chemistry Mass Spectrometry Service and the Advanced Chemical Equipment and Instrumentation Facility at the Faculty of Chemistry, Adam Mickiewicz University in Poznan. Elemental analyses were determined by the Advanced Chemical Equipment and Instrumentation Facility at the Faculty of Chemistry, Adam Mickiewicz University in Poznan.

Crystallography

Single crystals of **4** and **5** were obtained at room temperature from ethyl acetate:*n*-hexane solution. A summary of structure determination is given in Table 3. Intensity data were collected with a Kuma Diffraction KM4-CCD diffractometer using graphite-monochromated Mo K_α radiation. All structures were solved by direct methods with SHELXS97 and were refined with SHELXL97 by full-matrix least-squares based on F^2 [24]. All non-hydrogen atoms were refined anisotropically. Hydrogens at amine N atoms were located on an electron density

Table 3 X-ray experimental details of **4** and **5**

	4	5
Formula	$C_{16}H_{12}N_6$	$C_{16}H_{14}N_6$
FW	288.32	290.33
Crystal system	Monoclinic	Monoclinic
Space group	$P2_1/n$	$P2_1/n$
a (Å)	12.0756(4)	11.963(1)
b (Å)	7.4357(3)	7.7716(8)
c (Å)	16.1624(6)	16.241(2)
β (deg)	101.664(3)	103.31(1)
V (Å^3)	1,421.26(9)	1,469.5(3)
Z	4	4
T (K)	130(2)	140(2)
D_c (g/cm^3)	1.347	1.312
μ (cm^{-1})	0.087	0.084
Θ_{max} (deg)	26.4	26.4
R_1 (obs. data)	0.035	0.034
wR_2 (obs. data)	0.094	0.085
Independ. refs.	2,890	2,998
Refs. $I > 2\sigma(I)$	2,199	2,389

difference map and refined isotropically. The other H atoms were generated geometrically, with C–H = 0.93–0.98 Å, and refined as riding on their carriers, with $U_{iso}(H) = 1.2U_{eq}(C)$. Details on data collection and refinement, fractional atomic coordinates, anisotropic displacement parameters, and full list of bond lengths and angles in CIF format have been deposited at the Cambridge Crystallographic Data Centre. CCDC 783702 for **4** and CCDC 783703 for **5** contain the crystallographic data for this paper. Copy of the data can be obtained, free of charge, via http://www.ccdc.cam.ac.uk/conts/retrieving.html, or from the Cambridge Crystallographic Data Centre, 12 Union Road, Cambridge, CB2 1EZ, UK; fax: +44-1223-336033; or e-mail: deposit@ccdc.cam.ac.uk.

Quantum mechanical calculations

The conformational study process of **5** and **5-Na** is described in details in the Supplementary Material. The condensed Fukui functions and condensed softness (see references in the Supplementary Material) were obtained from single-point calculations on the optimized disodium salt structures of **5** (**5-Na**) with the 6-31G(d,p) basis set, using restricted B3LYP for neutral systems and unrestricted U-B3LYP hybrid functional for the corresponding cation and anion calculations. B3LYP functional appears to be reliable in f_k^-, f_k^+, and f_k^0 indices calculations [25]. All calculations were performed using the PC GAMESS/Firefly 7.1.E program [26].

2-[(3-Pyridylmethyl)amino]-3-[(3-pyridylmethylidene)-amino]-2(Z)-butene-1,4-dinitrile (**4**, $C_{16}H_{12}N_6$)

Two drops of CF_3COOH were added to 3.0 g **3** (15.1 mmol) and 2.4 g 3-pyridinecarboxaldehyde (22.6 mmol) dissolved in 60 cm^3 methanol. The mixture was stirred for 72 h. Precipitated solid was collected by vacuum filtration and washed with methanol and diethyl ether to give 2.6 g **4** as a yellow solid (60%). Recrystallization from ethyl acetate:*n*-hexane afforded 1.42 g yellow crystals (33%). M.p.: 206–208 °C; ^{1}H NMR (300 MHz, DMSO-d_6): δ = 9.19 (d, ^4J = 1.5 Hz, 1H, pyridine-H), 8.82 (bs, 1H, NH), 8.65 (dd, 1H, ^3J = 5.0 Hz, ^4J = 2.0 Hz, pyridine-H), 8.59 (d, 1H, ^4J = 2.0 Hz, pyridine-H), 8.53 (dd, 1H, ^3J = 5.0 Hz, ^4J = 1.5 Hz, pyridine-H), 8.41 (d, 1H, ^3J = 8.0 Hz, pyridine-H), 8.37 (s, 1H, N = CH), 7.79 (dt, 1H, ^3J = 8.0 Hz, ^4J = 2.0 Hz, pyridine-H), 7.50 (dd, 1H, ^3J = 8.0 Hz, ^3J = 5.0 Hz, pyridine-H), 7.43 (dd, 1H, ^3J = 8.0 Hz, ^3J = 4.5 Hz, pyridine-H), 4.68 (d, 2H, ^3J = 3.5 Hz, CH_2) ppm; ^{13}C NMR (75 MHz, DMSO-d_6): δ = 153.4, 151.8, 150.4, 148.8, 148.7, 135.6, 135.1, 133.8, 131.1, 128.7, 123.8, 123.8, 113.4, 113.0, 103.3, 46.9 (CH_2) ppm; MS (CI, NH_3): m/z = 289 (M+H$^+$); HRMS calcd for $C_{16}H_{13}N_6$ 289.1202, found 289.1205.

2,3-Bis[(3-pyridylmethyl)amino]-2(Z)-butene-1,4-dinitrile (**5**, $C_{16}H_{14}N_6$)

To 3.33 g **4** (11.5 mmol) suspended in 110 cm^3 methanol, 520 mg $NaBH_4$ (13.9 mmol) was added in three portions and stirred. After the addition was complete, the mixture was stirred for another 30 min and poured into 300 cm^3 ice-water mixture to form a precipitate. Filtration, drying under vacuum, and chromatography (dichloromethane:methanol, 10:1) afforded **5** as a yellow oil. Recrystallization from ethyl acetate:hexane afforded 1.50 g yellow crystals (45%). M.p.: 103–106 °C; ^{1}H NMR (300 MHz, DMSO-d_6): δ = 8.51 (s, 2H, 2 pyridine-H), 8.49 (hidden d, 2H, ^4J = 2.0 Hz, 2 pyridine-H), 7.68 (dt, 2H, ^3J = 8.0 Hz, ^4J = 2.0 Hz, 2 pyridine-H), 7.39 (dd, 2H, ^3J = 8.0 Hz, ^3J = 5.0 Hz, 2 pyridine-H), 6.05 (t, 2H, ^3J = 6.0 Hz, 2 NH), 4.30 (d, 4H, ^3J = 6.0 Hz, 2 CH_2) ppm; ^{13}C NMR (75 MHz, DMSO-d_6): δ = 148.9, 148.6, 135.2, 134.4, 123.6, 115.2, 109.9, 46.5 (2 CH_2) ppm; MS (CI, NH_3): m/z = 291 (M+H$^+$); HRMS calcd for $C_{16}H_{15}N_6$ 291.1358, found 291.1368.

2,3-Bis[methyl(3-pyridylmethyl)amino]-2(Z)-butene-1,4-dinitrile (**6**, $C_{18}H_{18}N_6$)

To 40 cm^3 dimethylformamide at −30 °C, 265 mg NaH (60% dispersion in mineral oil, 6.6 mmol) was added and stirred for 30 min. Further 960 mg **5** (3.31 mmol) in 5 cm^3 dimethylformamide was added within 30 min and stirred at −30 °C for 1.5 h. Finally, 0.59 cm^3 Me_2SO_4 (6.95 mmol) in 2 cm^3 dimethylformamide was added within 40 min at −10 °C. The mixture was stirred for 1.5 h and carefully poured into 100 cm^3 water-crushed ice mixture. The

aqueous layer was extracted with EtOAc (4 × 150 cm^3). The combined organic layers were washed with $NaHCO_3$ solution and water. Evaporation and chromatography (dichloromethane:methanol 10:1) afforded 147 mg (13%) **6** as a brown oil. $R_f = 0.19$ (ethyl acetate:methanol 5:1); MS (ESI): $m/z = 317$ ($M - H^-$), 341 ($M+Na^+$).

3,6-Bis(4-fluorobutoxy)benzene-1,2-dicarbonitrile (**7**, $C_{16}H_{18}F_2N_2O_2$)

To a well-stirred slurry of 0.808 g 2,3-dicyanohydroquinone (5.04 mmol) and 0.484 g NaH (60% dispersion in mineral oil, 10.08 mmol) in 25 cm^3 dimethylformamide cooled to 0 °C, 1.562 g 4-bromo-1-fluorobutane (10.08 mmol) was added after 1.5 h. The solution was heated at 50 °C for 24 h. The reaction contents were poured into 65 cm^3 water, and the suspension was vigorously stirred. The resulting white-cream solid was filtered and next suspended in 100 cm^3 methanol keeping under reflux. The filtration of the white solid afforded 1.447 g (92%) **7**. M.p.: 179–183 °C; $R_f = 0.82$ (tetrahydrofuran:methanol 1:1); UV (methanol): λ_{max} (log ε) = 226 (4.18), 350 (3.51) nm; ^{1}H NMR (300 MHz, DMSO-d_6): $\delta = 7.62$ (s, 2H, H-4, H-5), 4.51 (dt, 4H, $^2J_{HF} = 47.5$ Hz, $^3J = 5.5$ Hz, 2 CH_2F), 4.20 (t, 4H, $^3J = 6.0$ Hz, 2 CH_2O), 1.74–1.85 (m, 8H, 2 CH_2CH_2) ppm; ^{13}C NMR (75 MHz, DMSO-d_6): $\delta = 154.8$, 120.6, 113.5, 102.8, 83.5 (d, $^1J_{CF} = 161.5$ Hz), 69.3, 26.4 (d, $^2J_{CF} = 19.5$ Hz), 24.3 ppm; MS (CI, NH_3): $m/z = 326$ ($M+NH_4^+$); HRMS calcd for $C_{16}H_{22}N_3O_2F_2$ 326.1680, found 326.1683.

1,4,8,11,15,18-Hexakis(4-fluorobutoxy)-22,23-bis[methyl-(3-pyridylmethyl)amino]tribenzo[b,g,l]porphyrazinato-zinc(II) (**8**, $C_{66}H_{72}F_6N_{12}O_6Zn$)

To 2 cm^3 pentanol 65 mg **6** (0.20 mmol), 414 mg **7** (1.43 mmol), 300 mg $Zn(OAc)_2$ (1.63 mmol), and 0.244 cm^3 1,8-diazabicyclo[5.4.0]undec-7-ene (1.63 mmol) were added and heated under reflux for 23 h. Evaporation and chromatography (dichloromethane:methanol 25:1–15:1) afforded 25 mg greyish-blue **8** (9%) as a thin film. Further purification by means of PTLC afforded 8 mg (3%). $R_f = 0.29$ (dichloromethane:methanol 8:1); UV–Vis (dichloromethane:methanol 1:1): λ_{max} (log ε) = 332 (4.24), 730 (4.36) nm; ^{1}H NMR (400 MHz, pyridine-d_5): $\delta = 9.06$ (d, 2H, $^4J = 2.0$ Hz, 2 pyridine-2′H), 8.52 (dd, 2H, $^3J = 4.5$ Hz, $^4J = 1.5$ Hz, 2 pyridine-6′H), 7.89 (dt, 2H, $^3J = 8.0$ Hz, $^4J = 2.0$ Hz, 2 pyridine-4′H), 7.87 (s, 2H, 18-H, 19-H), 7.84 (d, 2H, $^3J = 8.5$ Hz, 2 Ar–H), 7.67 (d, 2H, $^3J = 8.5$ Hz, 2 Ar–H), 7.07 (dd, 2H, $^3J = 8.0$, Hz, $^3J = 4.5$ Hz, 2 pyridine-5′H), 6.20 (s, 4H, 2 CH_2), 5.13–5.18 (hidden m, 8H, 4 OCH_2), 4.65 (dt, 4H, $^2J_{HF} = 47.5$ Hz, $^3J = 6.0$ Hz, 2 CH_2F), 4.63 (dt, 4H, $^2J_{HF} = 47.5$ Hz, $^3J = 6.0$ Hz, 2 CH_2F), 4.63 (t, 4H, $^3J = 7.0$ Hz, 2 OCH_2), 4.58 (dt, 4H, $^2J_{HF} = 47.0$ Hz, $^3J = 6.0$ Hz, 2 CH_2F), 4.06 (s, 6H, 2 CH_3), 2.46–2.32 (m, 12H, 6 OCH_2CH_2), 1.98–2.26 (m, 12H, 6 CH_2CH_2F) ppm; ^{19}F NMR (376 MHz, pyridine-d_5): $\delta = -140.99$ (m), -141.04 (m), -141.21 (m) ppm; MS (MALDI): $m/z = 1307.592$ ($M+H^+$).

[1,4,8,11,15,18,22,25-Octakis(4-fluorobutoxy)phthalocyanato]zinc(II) (**9**, $C_{64}H_{72}F_8N_8O_8Zn$) was isolated as a side-product. $R_f = 0.32$ (dichloromethane:methanol 10:1); UV–Vis (dichloromethane:methanol 1:1): λ_{max} (log ε) = 328 (4.86), 663 (4.74), 738 (5.36), 822 (4.23) nm; ^{1}H NMR (400 MHz, pyridine-d_5): $\delta = 7.83$ (s, 8H, H-2, H-3, H-9, H-10, H-16, H-17, H-23, H-24), 5.08 (t, 16H, $^3J = 6.5$ Hz, 8 OCH_2), 4.62 (dt, 16H, $^2J_{HF} = 47.5$ Hz, $^3J = 6.0$ Hz, 8 CH_2F), 2.38 (p, $^3J = 7.0$ Hz, 16H, 8 OCH_2CH_2), 2.15 (dp, 16H, $^3J_{HF} = 25.5$ Hz, $^3J = 7.0$ Hz, 8 CH_2CH_2F) ppm; ^{19}F NMR (376 MHz, pyridine-d_5): $\delta = -139.97$ (m) ppm; ^{13}C NMR (100 MHz, pyridine-d_5): $\delta = 153.24$, 151.97, 128.65, 119.43, 84.4 (d, $^1J_{CF} = 163.0$ Hz), 72.16, 27.8 (d, $^2J_{CF} = 20.0$ Hz), 26.2 (d, $^3J_{CF} = 5.0$ Hz) ppm; MS (MALDI): $m/z = 1\ 297.572$ ($M+H^+$).

General procedure for UV–Vis titrations of tribenzoporphyrazine ***8***

CH_3OH:CH_2Cl_2 (1:1) solution of known concentration of porphyrazine **8** was subjected to UV–Vis titrations with CH_3OH:CH_2Cl_2 (1:1) solutions of varying concentrations (0, 0.01, 0.1, 0.5, 1 molar equiv.) of $PdCl_2(C_6H_5CN)_2$. Blank UV–Vis spectra (in the absence of metal salt) were run for **8** to determine any solvent effect (of which there were none). Blank UV–Vis spectra (in the absence of tribenzoporphyrazine **8**) were also run for the metal salt to make sure that there was no significant absorbance in the window of interest (300–850 nm).

Acknowledgments This study was supported in part by Polish Ministry of Science and Higher Education grant no. N405 031 32/2052. T.G. thanks Professor A.G.M. Barrett from Imperial College London and Professor S. Sobiak from Poznan University of Medical Sciences for supporting his studies. The authors thank Mrs B. Kwiatkowska for excellent technical assistance. Z.D. thanks MSc A. Maruszewski for preparation of input data for computational study.

References

1. Begland RW, Hartter DR, Jones FN, Sam DJ, Sheppard WA, Webster OW, Weigert FJ (1974) J Org Chem 39:2341
2. Ohtsuka Y (1976) J Org Chem 41:629
3. Beall LS, Mani NS, White AJP, Williams DJ, Barrett AGM, Hoffman BM (1998) J Org Chem 63:5806
4. Fuchter MJ, Beall LS, Baum SM, Montalban AG, Sakellariou EG, Mani NS, Miller T, Vesper BJ, White AJP, Williams DJ, Barrett AGM, Hoffman BM (2005) Tetrahedron 61:6115

5. Goslinski T, Zhong C, Fuchter MJ, Stern CL, White AJP, Barrett AGM, Hoffman BM (2006) Inorg Chem 45:3686
6. Al-Azmi A, Elassar AZA, Booth BL (2003) Tetrahedron 59:2749
7. Kubota Y, Shibata T, Babamoto-Horiguchi E, Uehara J, Funabiki K, Matsumoto S, Ebihara M, Matsui M (2009) Tetrahedron 65:2506
8. Beletskaya I, Tyurin VS, Tsivadze AY, Guilard R, Stern C (2009) Chem Rev 109:1659
9. Toma HE (2008) Curr Sci India 95:1202
10. Kobayashi N, Muranaka A, Nemykin VN (2001) Tetrahedron Lett 42:913
11. Cheng KF, Thai NA, Grohmann K, Teague LC, Drain CM (2006) Inorg Chem 45:6928
12. Haas M, Liu SX, Neels A, Decurtins S (2006) Eur J Org Chem 5467
13. Donzello MP, Viola E, Cai XH, Mannina L, Ercolani C, Kadish KM (2010) Inorg Chem 49:2447
14. Mørkved EH, Andreassen T, Novakova V, Zimcik P (2009) Dyes Pigm 82:276
15. Ojaimi ME, Habermeyer B, Gros CP, Barbe JM (2010) J Porphyr Phthalocyanines 14:469
16. Goslinski T, Tykarska E, Szczolko W, Osmalek T, Smigielska A, Walorczyk S, Zong H, Gdaniec M, Hoffman BM, Mielcarek J, Sobiak S (2009) J Porphyr Phthalocyanines 13:223
17. Cook AH, Linstead RP (1937) J Chem Soc 929
18. Forsyth TP, Bradley D, Williams G, Montalban AG, Stern CL, Barrett AGM, Hoffman BM (1998) J Org Chem 63:331
19. Dwyer TJ, Jasien PG (1996) J Mol Struct (Theochem) 363:139
20. Hemelsoet K, Van Speybroeck V, Waroquier M (2007) Chem Phys Lett 444:17
21. Bilgin A, Ertem B, Gök Y (2009) Dyes Pigm 80:187
22. Ogunsipe A, Maree D, Nyokong T (2003) J Mol Struct 650:131
23. Lide DR (ed) (1997) CRC handbook of chemistry and physics, 78th edn. CRC, Boca Raton
24. Sheldrick GM (2008) Acta Cryst A64:112
25. De Proft F, Martin JML, Geerlings P (1996) Chem Phys Lett 256:400
26. Granovsky AA, Firefly version 7.1.G. http://classic.chem.msu.su/gran/firefly/index.html